Koc. J. Sci. Eng., 8(2): (2025) 103-110 https://doi.org/10.34088/kojose.1476891

Kocaeli University

Kocaeli Journal of Science and Engineering

http://dergipark.org.tr/kojose

Investigation of the Atmospheric Turbulence Effects on Electro-Optical Reconnaissance Imaging Systems in the Marine Environment

B. Ferdi AKTAN [1,2,*], Elif KACAR [2,3]

[1] *Turkish Naval Research Center Command (TNRCC) Department of Electronic Warfare Research Department, Istanbul, Türkiye,* ***ORCID:*** *0000-0002-0346-1764*
[2] *Department of Electro-Optical Systems Engineering, Kocaeli University, Kocaeli, Türkiye*
[3] *Department of Physics, Kocaeli University, Kocaeli, Türkiye,* ***ORCID:*** *0000-0001-6682-0114*

Article Info

Research paper

Received : *May 1, 2024*
Accepted : *April 17, 2025*

Keywords

Electro-Optical Systems
Atmospheric Turbulence
DRI
NVIPM

Abstract

Atmospheric turbulence has a disruptive effect on the optical spectrum of the atmosphere in reconnaissance surveillance systems and especially in military laser operations. The main cause of atmospheric turbulence is that the atmosphere is composed of different gas and aerosol contents and is also subject to meteorological effects. To eliminate the disturbing effects of atmospheric turbulence, it is important to know the turbulence intensity. However, due to the complex structure of the atmosphere, knowing the atmospheric turbulence intensity is a difficult problem to solve. Due to the impossibility of turbulence measurements, especially at long distances, atmospheric turbulence prediction models have been developed. It is preferred to use estimated atmospheric turbulence values for fast information, when navigating over the sea because of this measurement difficulty. This study discusses, the effects of atmospheric turbulence on electro-optical reconnaissance and surveillance systems in the marine environment have been discussed. For this purpose, atmospheric turbulence predictions were made by collecting meteorological parameters in 4 different seasons of 2023 in the Marmara region and using the Sadot-Kopeika prediction model. Atmospheric turbulence measurements were also made at the same location and in the same time periods and compared with the prediction results. To investigate the effects of the atmospheric turbulence on the performance of electro-optical reconnaissance and surveillance systems, DRI (Detection-Recognation-Identification) analyzes of an electro-optical sensor were carried out with the NVIPM (Night Vision Integrated Performance Model) software. The predicted and the measured atmospheric turbulence values have been used in the DRI analyses. When the DRI analysis results were evaluated, it was seen that the performance percentages using the predicted atmospheric turbulence values were compatible with the performance percentages using the measured atmospheric turbulence values. Based on these results, it has been foreseen that by predicting atmospheric turbulence, countermeasures to be taken against turbulence can be developed and electro-optical reconnaissance surveillance systems can also gain the ability to estimate turbulence based on turbulence-induced distortions in the pixels of the cameras.

1. Introduction

Atmospheric turbulence is referred to as fluctuations in the refractive index of the atmosphere, also known as optical turbulence. These factors that cause changes in the refractive index of the atmosphere, whose unit is C_n^2, are changes in the atmosphere [1]. Changes in the refractive index of the atmosphere occur with changes in parameters such as temperature, humidity, wind intensity, pressure, the content of the gas mixture in the air, and aerosols suspended in the air. The most common effect of atmospheric turbulence on electro-optical imaging systems is the distortion of optical waves due to the change in the refractive index, resulting in blurring and fluctuation of the acquired images and consequently decreasing the image quality [2, 3-4]. At the same time, lasers, which have many military applications such as laser range clouds, high-power laser weapons, laser target markers, systems used in free space communication, are used in military applications in the optical spectrum of the possible electromagnetic spectrum, especially with electro-optical radiation surveillance systems. Turbulence causes the beam quality to

* Corresponding Author: burak62586@gmail.com

deteriorate, which leads to increased signal noise in free space communications and reduced ranges in applications such as high-power laser weapons and laser rangefinders, where the reflected beam from the target must be detected again. Due to the doubling of the same atmospheric path and greater exposure to atmospheric distortions, they create beam entanglement effects, especially in applications such as laser target designators, and increase the error range of precision shots [5]. Electro-optical behavioral surveillance systems have found a unique place in many fields such as medicine, industry, agriculture, astronomy and mobile device technologies, especially in the defense industry, especially in recent years, due to technologies such as fault detectors, cooling technologies, image processing and optics [6-8]. These systems specialize in detection at different wavelengths of the electromagnetic spectrum according to their areas of use. Electro-optical reconnaissance and surveillance systems are widely used in military applications because they work on the principle of detecting radiation from the source, passively providing environmental awareness to the user, without the need for an active electromagnetic broadcast like a radar [9].

Atmospheric turbulence is one of the important parameters in determining the performance limits of sensors, which is affected by the attenuation of the radiation from the target in the region to be detected along the atmospheric path it travels until it reaches the sensor of the electro-optical system. Although there are difficulties in determining the atmospheric turbulence parameter, it is a parameter that can be measured. At the same time, various estimation models have been developed to determine this parameter [10-13]. The theory of turbulence estimation developed by Kolmogorov tries to explain the statistical properties of turbulence [11]. G.I. Taylor hypothesized that turbulence has scale invariance between spatial scales [14]. In this hypothesis, it is assumed that where energy transfer occurs continuously, the basic statistical properties of turbulence will remain the same regardless of scale, even if observations are made at different scales of a turbulent flow [13]. In 1988, Dinstein, H. Zoabi, and N. S. Kopeika in 1990, Kopeika, Kogan, Israeli, and Dinstein and in 1992, Dan Sadot and Norman Kopeika [15] conducted studies that demonstrated the possibility of predicting atmospheric turbulence through meteorological measurements and developed two empirical models. One of the models is intended for practical use, while the other is more complex and includes additional parameters. The Sadot-Kopeika model predicts atmospheric turbulence using macrometeorological parameters rather than the more challenging-to-measure micrometeorological parameters. Additionally, macrometeorological parameters are influenced by the surrounding environment [15]. For instance, in a rural area with dense vegetation, a decrease in carbon dioxide levels due to photosynthesis, combined with the release of water vapor into the atmosphere, will lead to an increase in relative humidity and affect air temperature. Conversely, in a desert environment, the high temperature of desert sand will reduce humidity and affect temperature. Thus, the macroscopic approach encompasses not only atmospheric data but also environmental effects [15]. The practical model relies on standard meteorological parameters and shows a 90% correlation between the predicted and measured data. The complex model, in addition to standard parameters, also includes factors such as solar radiation flux and the concentration of aerosol particles per cubic meter [15].

There is not yet a precise theory that fully explains atmospheric turbulence. However, various theories and models have been developed to understand the nature of atmospheric turbulence and explain its effects [11-13].In this study, the Sadot-Kopeika model was used to predict atmospheric turbulence. The reason for selecting this model is its use of macro-meteorological parameters, which account for the effects of the marine environment on atmospheric turbulence predictions, thereby incorporating environmental factors while also relying on readily available fundamental meteorological parameters. Studies showing that the atmospheric turbulence predictions obtained by applying this semi-empirical model using standard meteorological data for different time periods of the day and year are 90% compatible with experimental measurement results [15], but studies have not been conducted in the marine environment in different seasons. For this reason, our atmospheric turbulence measurement and prediction studies were carried out with data collected in four seasons of the year.

The difficulty in measuring atmospheric turbulence makes it difficult to determine the performance of electro-optical systems. This has led to the need for atmospheric turbulence estimation. Especially in military applications, measured atmospheric turbulence values are used to evaluate the DRI (Detection, Recognition, Identification) performance of electro-optical reconnaissance surveillance systems. However, due to the difficulty in their measurement, especially when navigating over the sea, the use of predicted atmospheric turbulence values is preferred for fast information.

To investigate the effect of atmospheric turbulence on electro-optical reconnaissance imaging systems in the marine environment, meteorological data were collected, atmospheric turbulence measurements were made and images were taken with a short wavelength infrared camera at 10 meters above the sea surface on random days in four different seasons of the year 2023 in Istanbul/Tuzla. Atmospheric turbulence prediction values were calculated using the Sadot-Kopeika semi-empirical model and

compared with experimentally measured values. The measured and predicted atmospheric turbulence parameters were used to analyze the detection, recognition and identification range performance of an electro-optical imaging system, the thermal camera. The effects of atmospheric turbulence on surveillance systems have been discussed.

2. Materials and Methods

In this study, atmospheric turbulence measurements were made, meteorological data were collected for atmospheric turbulence prediction and the performance of the electro-optical system was analyzed with the obtained data.

The Scintec BLS450 Scintillometer atmospheric turbulence meter was used to measure atmospheric turbulence. The Scintillometer shown in Figure 1 (a) consists of a transmitter and receiver emitting an electromagnetic wave at 850 nm wavelength.

For the observation of atmospheric turbulence effects, a short-wavelength infrared (SWIR) NIT WIDY SENS 640 camera, shown in Figure 1 (b), was used. The SWIR camera has a resolution of 640x512 pixels, an InGaAs (Indium Gallium Arsenide) uncooled detector and can detect in the wavelength range of 0.9-1.7 micrometers.

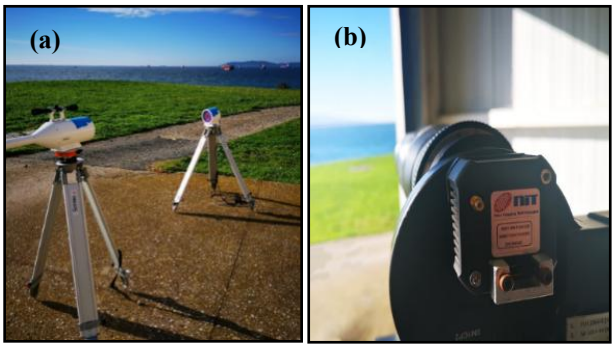

Figure 1. (a) Scintec BLS450 turbulence meter, **(b)** NIT WIDY SENS SWIR camera.

For meteorological measurements, the ORTANA METEOS 101 meteorological sensor and the ORTANA METEOS 151 visibility sensor shown in Figure 2 were used. The meteorological station can measure air temperature, relative humidity, precipitation intensity, precipitation type, wind speed, wind direction and air pressure.

Night Vision Integrated Performance Model (NVIPM) software was used for thermal camera detection, identification and identification analysis. The NVIPM software was developed by the US Army for the performance evaluation of electro-optical imaging systems.

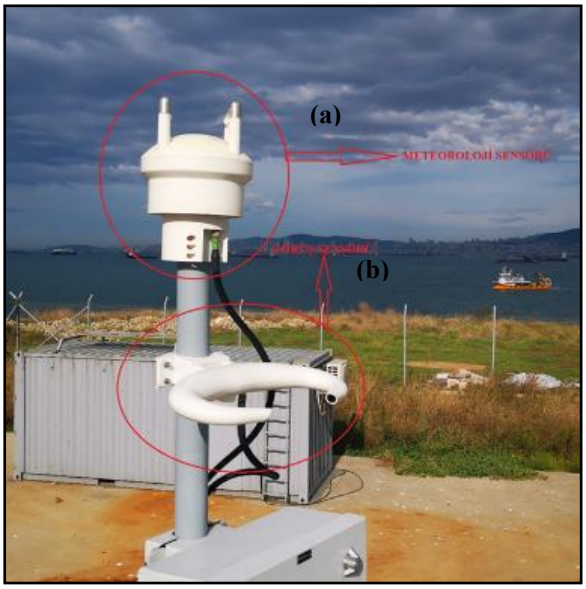

Figure 2. (a) Meteorological sensor, **(b)** vision sensor.

3. Atmospheric Turbulence Measurements and Predictions

The effects of atmospheric turbulence vary in different seasons of the year in different regions of the Earth. to examine the change of these effects in different seasons in the Marmara region of our country, 4 groups of meteorological data were collected for January, April, July and October of 2023. The days and time intervals when the data were collected are given in Table 1. Meteorological data collected at the specified times are given in Table 2. These data were used in atmospheric turbulence prediction calculations.

Table 1. Time intervals during which meteorological and atmospheric data are measured.

Code	Date	Time Intervals
JAN.23	January 27, 2023	14:02 - 15:02
APR.23	April 5, 2023	11:17 - 12:17
JUL.23	July 19, 2023	13:34 - 14:34
OCT.23	October 10, 2023	14:29 - 15:29

Atmospheric turbulence measurements were made on the dates and time intervals when meteorological measurements were made with turbulence receiver/transmitter units placed at a distance of approximately 1100 meters and at a height of approximately 10 meters above the sea surface in Sırttepe, Tuzla district of Istanbul. During the measurements, data were recorded at a rate of six recordings per minute. Figure 3 shows the placement of the transmitter and receiver of the turbulence meter on the map. The turbulence meter receiver, meteorological station and SWIR camera were placed in the

same location.

SWIR camera images were also taken at the same location at the times when meteorological measurements and atmospheric turbulence measurements were made. Figure 4 shows the SWIR camera images recorded in weak-moderate turbulence on JAN.23 , Figure 5 shows the SWIR camera images recorded in moderate turbulence on JUL.23 and Figure 6 shows the SWIR camera images recorded in moderate-high turbulence on OCT.23. In all three figures, (a) shows the camera images of the reference wind turbines at a distance of 30 km and (b) shows the camera images at a distance of 20 km. During the experimental studies on April 5, 2023, the atmospheric visibility dropped to 10 km and below, so the images of the reference wind turbines at distances of 20 km and 30 km could not be obtained.

The Sadot-Kopeika prediction model was used for atmospheric turbulence predictions to compare with experimentally measured atmospheric turbulence values [15]. The most important factor in the selection of this model is the use of macro-meteorological parameters defined in such a way that the effects of the marine environment are not independent of the atmospheric effects in atmospheric turbulence prediction calculations in the marine environment.

Figure 3. Satellite image of the study area.

Table 2. Meteorological data collected for the use in atmospheric turbulence prediction calculations.

Date	Temperature (^{0}C)	Humidity (%)	Optical Vision (km)	Pressure (hPa)	Wind Speed (m/s)	Wind Direction (^{0})
JAN.23	13	78	20 km	1008	6,3	184
APR.23	7	87	10 km	1013	5,8	262
JUL.23	29	48	20 km	1019	9,7	119
OCT.23	19	65	20 km	1024	9,9	92

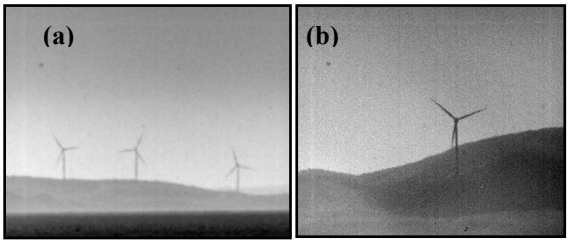

Figure 4. SWIR camera images taken at a distances of **(a)** 30 km and (**b)** 20 km in weak to moderate turbulence on JAN.23.

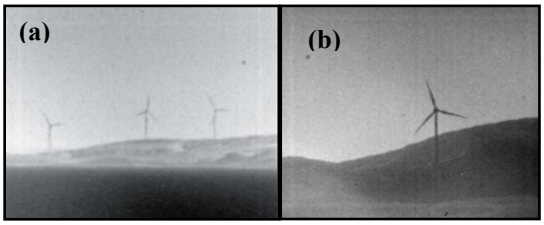

Figure 5. SWIR camera images taken at distances of **(a)** 30 km and **(b)** 20 km in moderate turbulence on JUL.23.

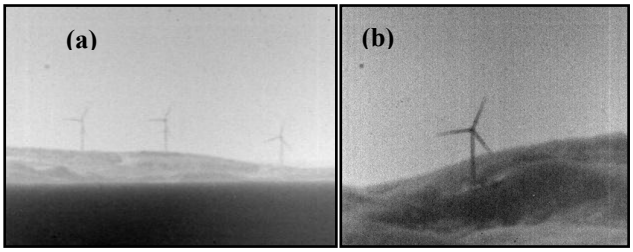

Figure 6. SWIR camera images taken at distances of **(a)** 30 km and **(b)** 20 km in moderate to high turbulence on OCT.23.

In addition to the fact that atmospheric turbulence prediction results can be calculated in a way that includes environmental factors, the easy availability of the basic meteorological parameters used in this model is also a reason for preference. Atmospheric turbulence coefficient in this semi-empirical model C_n (in units of $m^{-2/3}$) is given by [15];

$$C_n^2 = a_1 W + b_1 T + c_1 RH + c_2 RH^2 + c_3 RH^3 + d_1 WS + d_2 WS^2 + d_3 WS^3 + e \quad (1)$$

where *W is* temporal hour weight (relative weight), *T* is the temperature in kelvin, *RH is the* relative humidity, *WS* is the wind speed. The hour weight coefficients are given in Table 3. The hour weight coefficient is a coefficient that considers sunrise and sunset times to be weak in terms of turbulence and midday to be relatively strong. The regression coefficients a_1 , b_1 , c_1 , c_2 , c_3 , d_1 , d_2 , d_3 and *e* in Equation (1) are given in Table 4.

Table 3. Values of relative weight for particular temporal hour intervals used in the model [15].

Temporal Hour Interval *TH* [h]	**Relative Weight *W* [-]**
up to -4	0.11
-3 to -2	0.11
-2 to -1	0.07
-1 to 0	0.08
0 to 1	0.06
1 to 2	0.05
2 to 3	0.10
3 to 4	0.51
4 to 5	0.75
5 to 6	0.95
6 to 7	1.00
7 to 8	0.90
8 to 9	0.80
9 to 10	0.59
10 to 11	0.32
11 to 12	0.22
12 to 13	0.08
over 13	0.13

When the relationship between atmospheric turbulence and time of day is analyzed, it is observed that turbulence is higher at noon and shows lower values close to sunrise and sunset [15]. Therefore, in the turbulence estimation to account for the effect of the sun-dependent time at the time of estimation, the *TP* coefficient is calculated from

$$TP = \frac{|t_{sunrise} - t_{sunset}|}{12} . \quad (2)$$

Using this *TP* coefficient, the temporal hour interval *TH* is calculated from;

$$TH = \frac{t - t_{sunrise}}{TP} \quad (3)$$

to determine the temporal hour weight *W*.

Table 4. The regression coefficients used in the model [15].

Regression Coefficients	
a_1	3.8E-14
b_1	2.0E-15
c_1	-2.8E-15
c_2	2.9E-17
c_3	-1.1E-19
d_1	-2.5E-15
d_2	1.2E-15
d_3	-8.5E-17
e	-5.3E-13

Experimentally measured atmospheric turbulence values and atmospheric turbulence predictions obtained with the semi-empirical model using collected meteorological data are given in Table 5. Each of the measured atmospheric turbulence values was added to the table by averaging 360 data points measured at the specified time of day. The atmospheric turbulence data measured on JAN.23 ranges from 1.93×10^{-15} $m^{-2/3}$ to 1.30×10^{-15} $m^{-2/3}$, with an average value of 1.63×10^{-15} $m^{-2/3}$, which can be considered as weak-moderate turbulence. The atmospheric turbulence values on APR.23 and JUL.23 can be considered as moderate turbulence, and the atmospheric turbulence value on OCT.23 can be considered as moderate-high turbulence.

Table 5. Measured and predicted atmospheric turbulence values.

Date	**Measured** C_n^2 (m)$^{-2/3}$	**Predicted** C_n^2 (m)$^{-2/3}$
JAN.23	$1{,}63 \times 10^{-15}$	$1{,}00 \times 10^{-14}$
APR.23	$1{,}25 \times 10^{-14}$	$1{,}00 \times 10^{-14}$
JUL.23	$1{,}48 \times 10^{-14}$	$1{,}00 \times 10^{-13}$
OCT.23	$1{,}04 \times 10^{-13}$	$1{,}00 \times 10^{-13}$

4. Results and Discussion

In this study, the effects of the atmospheric turbulence on the electro-optical reconnaissance imaging systems in the marine environment were investigated. For this purpose, the performance of an electro-optical system was analyzed using both experimentally measured and empirically modeled atmospheric turbulence data. For the DRI (Detection, Recognition, Identification) analysis, which involves the prediction of the detection, recognition and identification ranges of an electro-optical system's sensor for a target, a cooled sensor with a resolution of 640x512 pixels that can detect in the wavelength range of 0.3-13 micrometers was defined. Atmospheric data for the measured days were used to model the atmosphere and the Navy Maritime Aerosol model in the MODTRAN algorithm

was used for aerosol modeling. Among the atmospheric models, Mid-Latitude Winter for cold days and Mid-Latitude Summer for hot days were selected. The atmospheric visibility parameter was assumed to be >30 km so that the DRI analysis could be compared at equal ranges. Sensor pixel pitches were defined as 15 micrometers both horizontally and vertically. For the detection camera parameters, an optical aperture of 100 mm and a focal length of 300 mm were defined, and the temperature of the optics was chosen to be equal to the ambient temperature based on the ambient temperature of that day. The target temperature was set to give a contrast temperature of 3°C for each day from the atmospheric temperature, and the target size was set as 3x3 meters. Observer parameters were chosen using an altitude of 10 meters above sea level and a range of 30 km.

DRI analyses were performed for the days when meteorological measurements and atmospheric turbulence forecasts were made and the effect of atmospheric turbulence was analyzed. As a result of the DRI analyses performed using the measured atmospheric turbulence values, the performance (detection percentage) graphs according to the detection range, recognition range and identification range obtained on the measurement days are given in Figure 7, Figure 8 and Figure 9, respectively. As a result of the DRI analyses performed using the predicted atmospheric turbulence values, the performance (detection percentage) graphs according to the detection range, recognition range and identification range obtained on meteorological measurement days are given in Figure 10, Figure 11 and Figure 12, respectively.

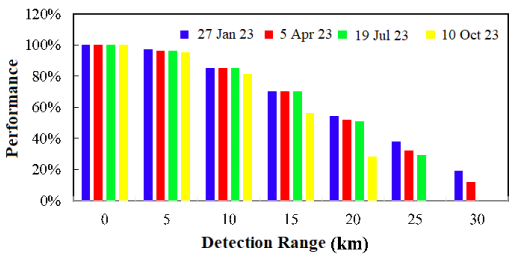

Figure 7. Measured C_n^2 for comparative detection ranges.

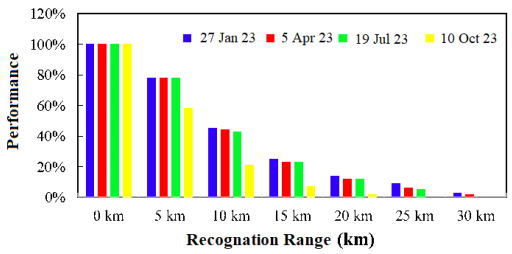

Figure 8. Measured C_n^2 for comparative recognition ranges.

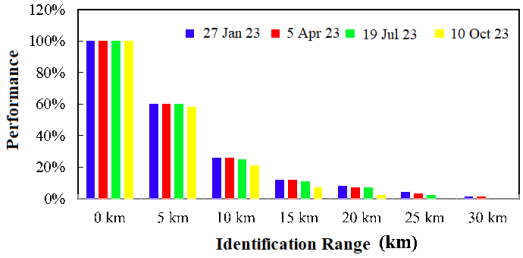

Figure 9. Measured C_n^2 for comparative identification ranges.

Considering the precision of the meteorological measurement device (±0.2 degrees Celsius temperature, ±2% relative humidity, ±0.3 m/s wind speed) [16], the aeorosol content of the atmosphere, the margin of error of the turbulence measurement device [17], and the uncertainties due to the atmospheric transmittance algorithm MODTRAN during the DRI analysis [18], it can be assumed that the measured atmospheric turbulence and the predicted atmospheric turbulence values overlap up to the over-the-horizon range (20 km).

Detection range is the maximum distance between the target and the sensor at which the target is first recognized as an object in the image by filling the minimum number of pixels and at which the user or the detection algorithm can make the decision "there is a target here". For this reason, detection ranges are generally higher than identification and characterization ranges, although ranges vary depending on weather conditions. However, this relative increase in the detection distance also leads to situations where the cumulative effect of atmospheric turbulence is more clearly observed and differences occur. In this context, in these graphs using measured (Figure 8) and predicted (Figure 11) atmospheric turbulence data, there is a difference of less than 4% between the detection percentages (performance) by detection range, when evaluated at over-the-horizon range. If a similar evaluation is made by comparing the recognition (Figure 9 and Figure 12) and identification (Figure 10 and Figure 13) graphs, it can be concluded that the differences between the detection percentages are insignificant in terms of uncertainties and errors. Since the recognition and identification ranges are relatively lower than the detection ranges, they are relatively less affected than the detection ranges.

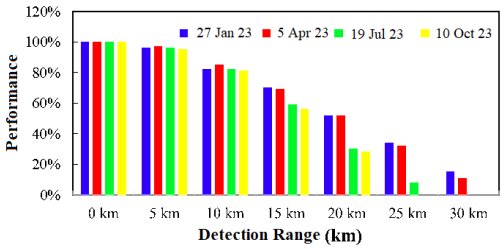

Figure 10. Predicted C_n^2 for comparative detection ranges.

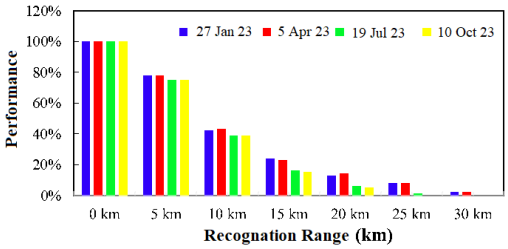

Figure 11. Predicted C_n^2 for comparative recognition ranges.

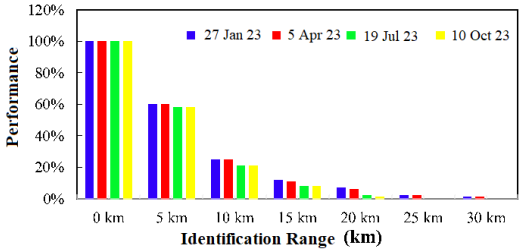

Figure 12. Predicted C_n^2 for comparative identification ranges.

4. Conclusions

Electro-optical sensors are used in many fields. Since the performance parameters of these sensors depend on atmospheric conditions, there is a need to define the performance criteria for that system in line with the needs when defining a system. When the system is realized, the performance criteria defined in the system design phase must be verified. However, since the electro-optical spectrum is inherently affected by meteorological conditions, it becomes difficult to verify the performance criteria. Atmospheric turbulence is one of the parameters that complicates this task and increases the uncertainty in the verification of the performance criteria. In this study, it is shown that atmospheric turbulence estimation can be made to approach the measured value by using meteorological data of the relevant time/day for the verification of performance criteria. The prediction can be done by directly fitting the atmospheric data into the prediction model, as in this study, or automatically by using image processing algorithms based on pixel-based distortions in the acquired image. The problems exposed to the sensor of an electro-optical surveillance system due to atmospheric turbulence estimation/approximation/ measurement can be reduced and thus performance losses due to atmospheric turbulence can be observed and prevented. Electro-optical sensors can be transformed into devices that can estimate atmospheric turbulence using image processing algorithms.

Declaration of Ethical Standards

The authors of this article declare that the materials and methods used in this study do not require ethical committee permission and/or legal-special permission.

Conflict of Interest

The authors declare that they have no known competing financial interests or personal relationships that could have appeared to influence the work reported in this paper.

References

[1] Xu M., Shao S., Weng N., Zhou L., Liu Q., Zhao Y., 2021. Atmospheric Optical Turbulence Characteristics Over the Ocean Relevant to Astronomy and Atmospheric Physics. Applied Sciences, **11**, 10548, pp. 1-13.

[2] Tunick A. D., 1998. The Refractive Index Structure Parameter/Atmospheric Optical Turbulence Model: CN2, Army Research Laboratory, USA.

[3] Hulea M., Tang X., Ghassemlooy Z. and Rajbhandari S., 2016. A Review on Effects of the Atmospheric Turbulence on Laser Beam Propagation An – Analytic Approach. 10th International Symposium on Communication Systems, Networks and Digital Signal Processing (CSNDSP), Prague, Czech Republic, pp. 1-6, doi: 10.1109/CSNDSP.2016.7573975.

[4] Beland R. R., 1993. Propagation through Atmospheric Optical Turbulence, The Infrared and Electro-Optical Systems Handbook, SPIE Optical Engineering Press, USA.

[5] Trichili, A., Cox, M., Ooi, B., Alouini, M.S. (2020). Roadmap to Free Space Optics. Journal of the Optical Society of America B. 37(11), 184-201.

[6] Künzner, N., Kushauer, J., Katzenbeißer, S., Wingender, K. (2010). Modern electro-optical imaging system for maritime surveillance applications. International WaterSide Security Conference, Carrara, İtalya, 3-5 Ekim 2010.

[7] Lahiri, B.B., Subramaniam, B., Jayakumar, T., Philip, J. (2012). Medical applications of infrared

thermography A review. Infrared Physics & Technology, (55), 221-235.

[8] Glavaš, H., Bobic, T., Dorić, D., Bozic Lenard, D. (2018). Infrared thermography camera protection in dairy farming management. Computers and Electronics in Agriculture, (157), 604-615.

[9] Hou, Fujin., Zhang, Yan., Zhou, Yong., Zhang, Mei., Bin, Lyu., Wu, J. (2022). Review on Infrared Imaging Technology. Sustainability, 14(18), 11161.

[10] Hudcova L., Wilfert O., 2017. Prediction of Atmospheric Turbulence on the Basis of Weather Conditions. 2017 Conference on Microwave Techniques (COMITE), Brno, Czech Republic, pp. 1-5, doi: 10.1109/COMITE.2017.7932305.

[11] Birnir B., 2013.The Kolmogorov-Obukhov theory of turbulence, Springer New York, NY, USA.

[12] Wei T., Willmarth W., 1988. Reynolds-Number Effects On The Structure Of A Turbulent Channel Flow, Journal of Fluid Mechanics, **204**, pp. 57-95.

[13] Zaman K. B. M. Q. and Hussain A. K. M. F, 1981. Taylor hypothesis and large-scale coherent structures, Journal of Fluid Mechanics, **112**, pp. 379-396.

[14] Taylor G. I., 1938. The Spectrum of Turbulence, Proceedings of The Royal Society of London A, **164**, pp. 476–490.

[15] Sadot D., Kopeika N. S., 1992. Forecasting Optical Turbulence Strength On The Basis Of Macroscale Meteorology and Aerosols: Models and Validation, Optical Engineering, **31**(2), pp. 200-212.

[16] ITS Weather Stations METEOS 101 Specifications.

[17] Kleissl J., Watts C.J., Rodriguez J.C., Naif S., Vivoni E. R., 2009. Scintillometer Intercomparison Study-Continued, Boundary-Layer Meteorol **130**, pp. 437–443.

[18] Ross V., Dion D., and St-Germain D., (2012). Experimental Validation of the MODTRAN 5.3 Sea Surface Radiance Model Using MIRAMER Campaign measurements, Applied Optics, **51** (13), pp. 2264-2276.